Electronic Supplementary Material (ESI) for Catalysis Science & Technology.

O-MoS_2/$Mn_{0.5}Cd_{0.5}S$ composites with enhanced activity for visible-light-driven photocatalytic hydrogen evolution

Xuanxuan Yang, Yu Guo, Yongbing Lou*, Jinxi Chen*

School of Chemistry and Chemical Engineering, Jiangsu Engineering Laboratory of Smart Carbon-Rich Materials and Device, Southeast University, Nanjing 211189, PR China

**Corresponding author.*

**E-mail address: chenjinxi@seu.edu.cn (J. Chen); lou@seu.edu.cn (Y. Lou);*

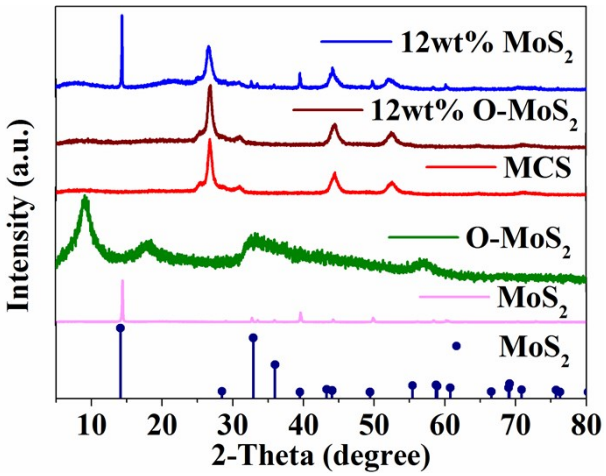

Fig. S1. XRD patterns of MoS_2, O-MoS_2 and their composites.

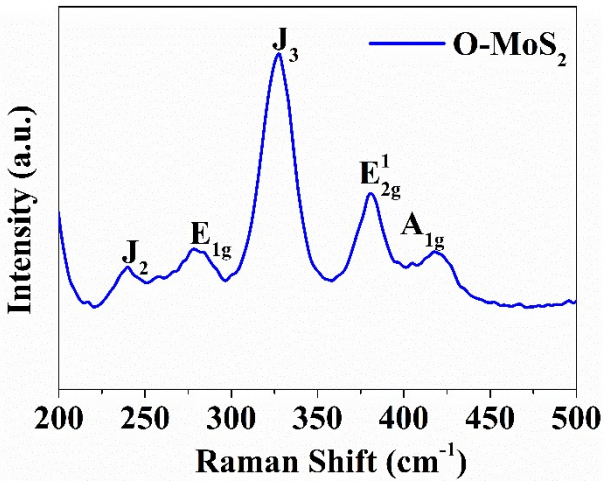

Fig. S2. Raman spectrum of O-MoS_2.

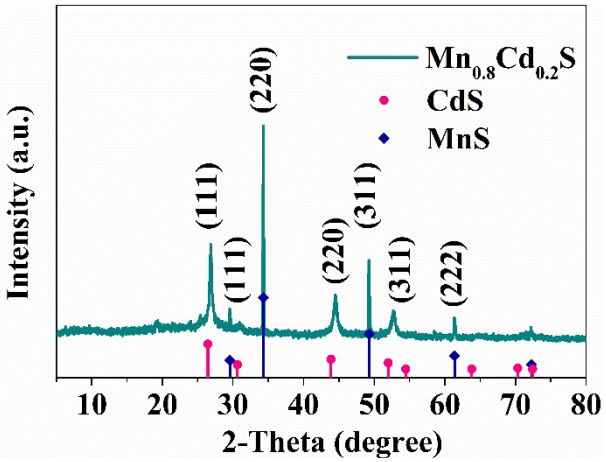

Fig. S3. XRD pattern of $Mn_{0.8}Cd_{0.2}S$ nanoparticles.

To further elucidate the phase structure of $Mn_{0.5}Cd_{0.5}S$, $Mn_{0.8}Cd_{0.2}S$ nanoparticles with a similar crystal phase are synthesized in the same condition (just increase the ratio

of Mn and Cd elements) and the crystallinity of them are investigated with XRD. As demonstrated, three sharp and noticeable diffraction peaks of all samples at 26.9°, 31.0°, 44.5° and 52.7° are assigned respectively to the (111), (200), (220) and (311) planes of cubic phase CdS (JCPDS No. 89-440), which is similar to that of $Mn_{0.5}Cd_{0.5}S$. Apart from that, the sample of $Mn_{0.8}Cd_{0.2}S$ displays four new features at about 29.6°, 34.3°, 49.3° and 61.3° (Fig.S3), which are separately matched with the (111), (220), (311) and (222) reflections of cubic α-MnS (JCPDS No. 89-4952). The result indicates that as-prepared $Mn_{0.5}Cd_{0.5}S$ solid solution is cubic phase.

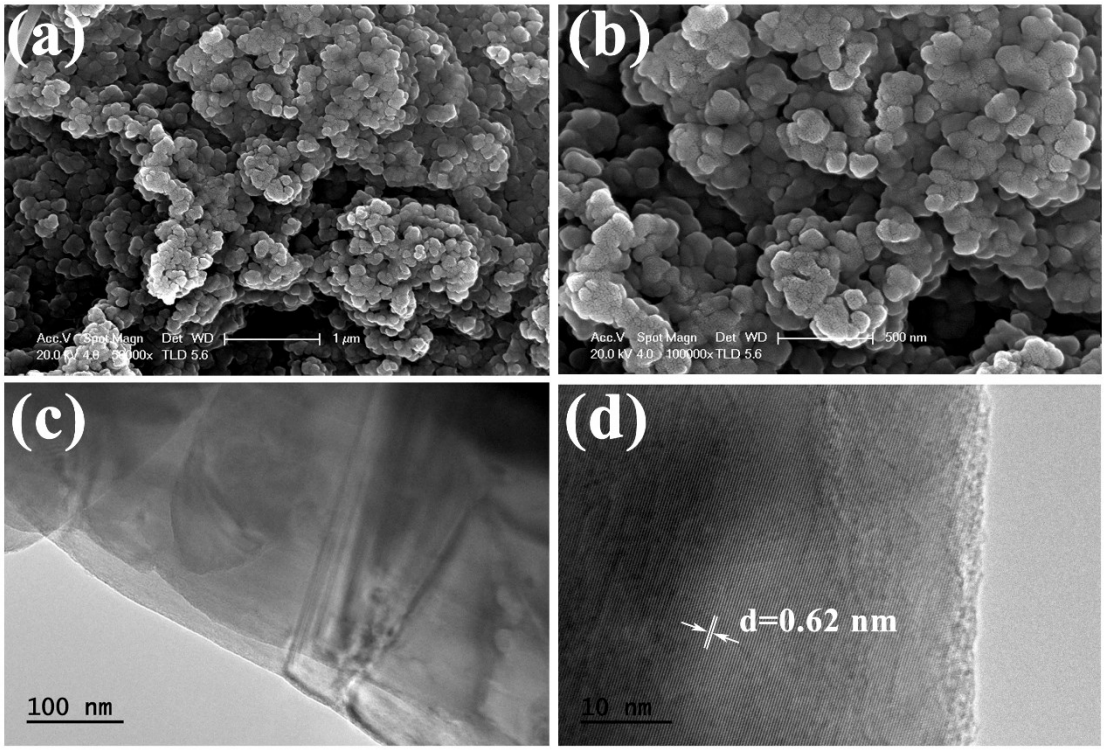

Fig. S4. SEM (a)(b) and TEM (c)(d)of MoS_2.

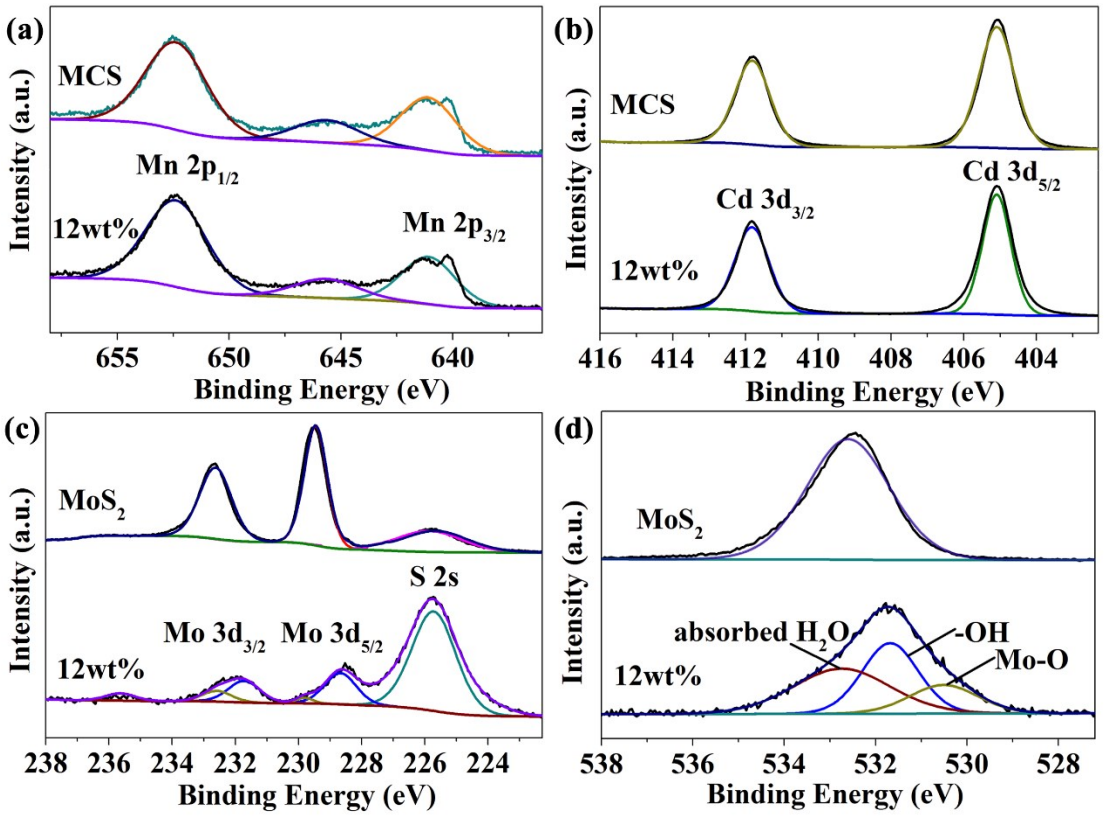

Fig. S5. XPS comparisons of $Mn_{0.5}Cd_{0.5}S$, MoS_2 and 12wt% O-MoS_2/ $Mn_{0.5}Cd_{0.5}S$.

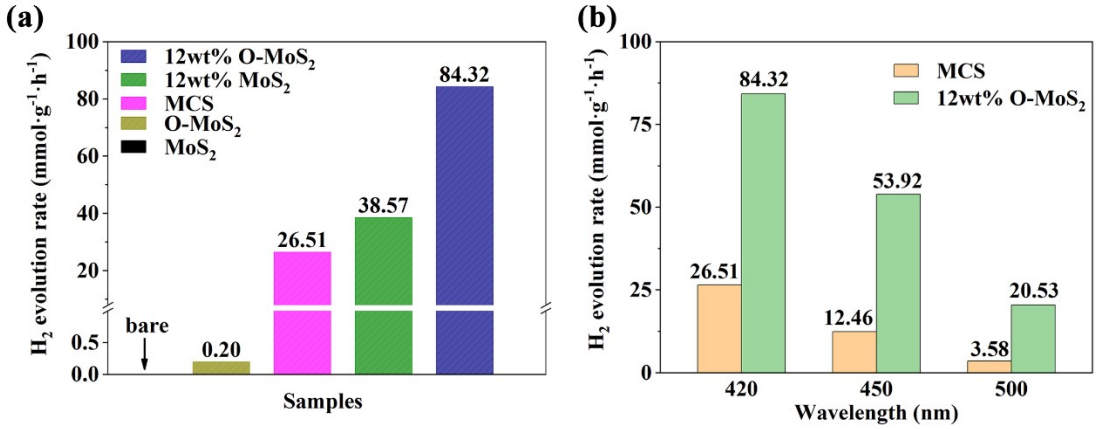

Fig. S6. Photocatalytic hydrogen evolution rates of composites (a) at 420 nm and (b) at different wavelengths.

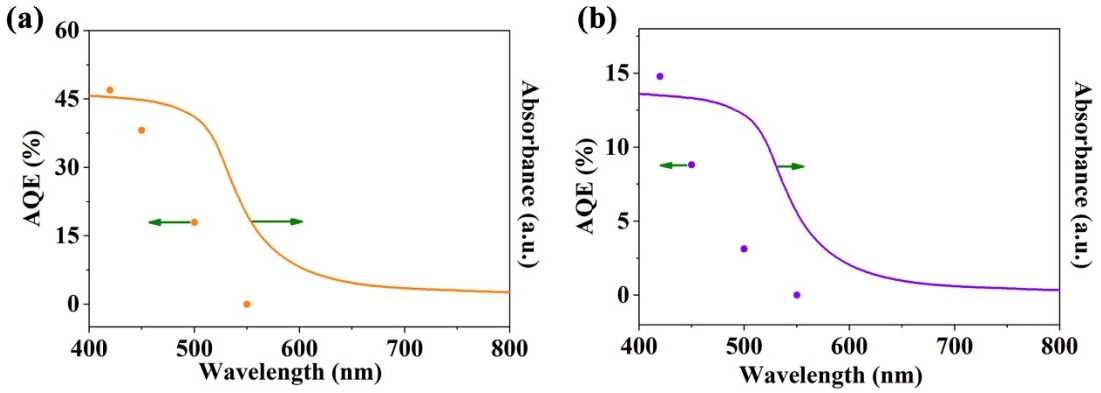

Fig. S7. The wavelength-dependent AQE of 12wt% O-MoS_2/$Mn_{0.5}Cd_{0.5}S$ and pristine $Mn_{0.5}Cd_{0.5}S$ for hydrogen evolution.

Table S1. The AQE values of $Mn_{0.5}Cd_{0.5}S$ and 12wt% O-MoS_2/$Mn_{0.5}Cd_{0.5}S$ at different wavelengths.

Sample	Wavelength (nm)	420	450	500	550
12wt%	Evolved H_2 ($mmol\ g^{-1}\ h^{-1}$)	84.32	53.92	20.53	0
	AQE (%)	46.92	38.14	17.94	0
$Mn_{0.5}Cd_{0.5}S$	Evolved H_2 ($mmol\ g^{-1}\ h^{-1}$)	26.51	12.46	3.58	0
	AQE (%)	14.79	8.81	3.13	0

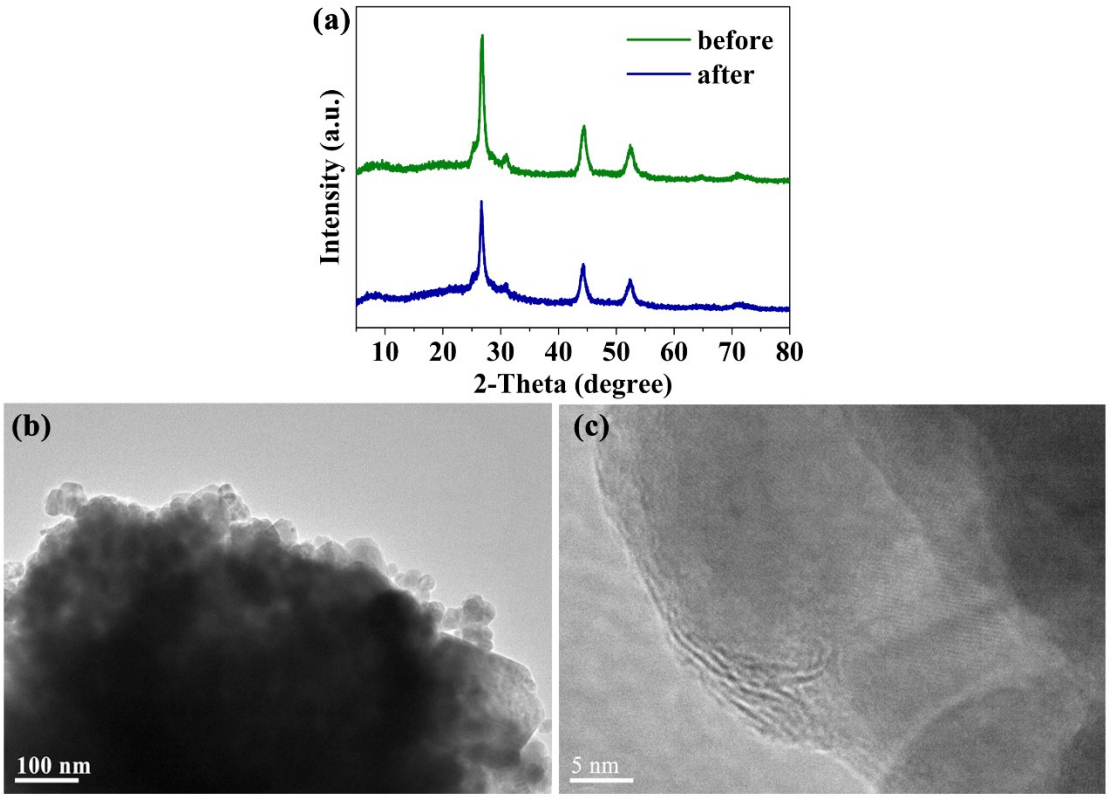

Fig. S8. (a) XRD patterns of 12wt% O-MoS_2/$Mn_{0.5}Cd_{0.5}S$ after reaction for 16 h under visible light irradiation (b) TEM and (c) HRTEM image of 12wt% O-MoS_2/ $Mn_{0.5}Cd_{0.5}S$ after reaction for 16 h under visible light irradiation.

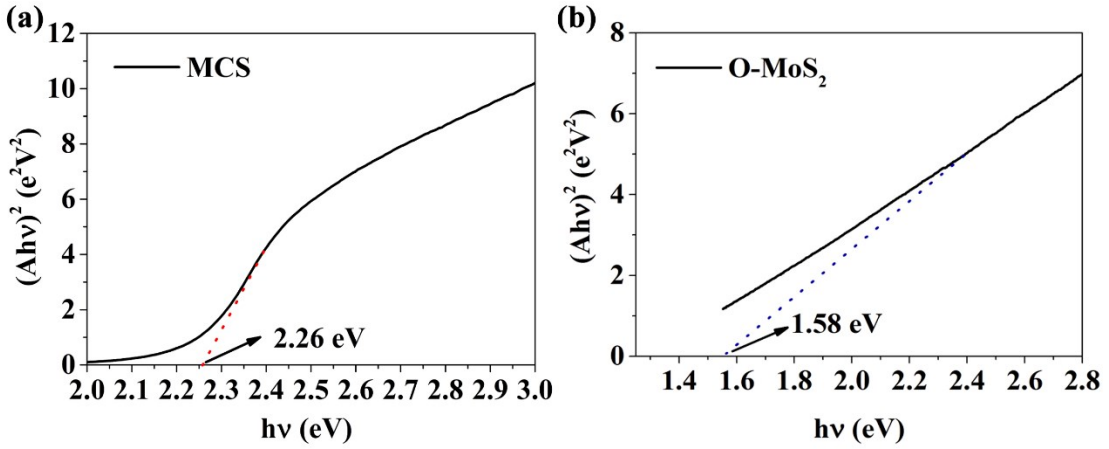

Fig. S9. (a) calculated bandgap of $Mn_{0.5}Cd_{0.5}S$ and (b) O-MoS_2.

Table S2. The data obtained from of time-resolved PL decay spectra fitted curves of

$Mn_{0.5}Cd_{0.5}S$ and 12wt% O-MoS_2/$Mn_{0.5}Cd_{0.5}S$.

Sample	T_1 (ns)	T_2 (ns)	T_3 (ns)	A_1 (%)	A_2 (%)	A_3 (%)	Avlifetime (ns)
$Mn_{0.5}Cd_{0.5}S$	0.93	3.48	17.59	29.16	53.11	17.73	5.24
12wt%	1.13	5.43	18.65	32.52	54.36	13.12	5.77

Table S3. Comparison on the hydrogen evolution rates of other Mn-Cd-S-based composites.

Photocatalyst	Sacrificial agents	Light source	Maximum rate (mmol g^{-1} h^{-1})	Reference
O-MoS_2/$Mn_{0.5}Cd_{0.5}S$	Na_2S/Na_2SO_3	$\lambda \geq 420$nm	84.32	This work
$Mn_{0.8}Cd_{0.2}S$	Na_2S/Na_2SO_3	$\lambda > 420$nm	3.56	[1]
$Mn_{0.5}Cd_{0.5}S$	Na_2S/Na_2SO_3	$\lambda > 400$nm	26.00	[2]
Pt/$Mn_{0.6}Cd_{0.4}S$	Lactic acid	$\lambda > 420$nm	2.25	[3]
MoS_2/$Mn_{0.25}Cd_{0.75}S$	Na_2S/Na_2SO_3	$\lambda > 400$nm	12.47	[4]
MoS_2/$Mn_{0.5}Cd_{0.5}S$	Na_2S/Na_2SO_3	$\lambda \geq 420$nm	9.82	[5]
MoS_2/$Mn_{0.8}Cd_{0.2}S$/MnS	Na_2S/Na_2SO_3	$\lambda \geq 420$nm	19.90	[6]
MoS_2/$Mn_{0.5}Cd_{0.5}S$/$Cu_{2-x}S$	Na_2S/Na_2SO_3	$\lambda \geq 420$nm	13.75	[7]
MoS_2/$Mn_{0.5}Cd_{0.5}S$/RGO	Na_2S/Na_2SO_3	Solar light	12.84	[8]
CuS/$Mn_{0.5}Cd_{0.5}S$	Na_2S/Na_2SO_3	$\lambda \geq 420$nm	106.84	[9]
CoS_x/$Mn_{0.5}Cd_{0.5}S$	Na_2S/Na_2SO_3	$\lambda > 420$nm	8.60	[10]
CoP_3/$Mn_{0.8}Cd_{0.2}S$	Na_2S/Na_2SO_3	$\lambda \geq 420$nm	29.53	[11]
CoP/$Mn_{0.5}Cd_{0.5}S$	Na_2S/Na_2SO_3	$\lambda \geq 420$nm	65.32	[12]
NiS/$Mn_{0.5}Cd_{0.5}S$	Na_2S/Na_2SO_3	$\lambda \geq 420$nm	8.39	[13]
g-C_3N_4/$Mn_{0.8}Cd_{0.2}S$	Na_2S/Na_2SO_3	$\lambda > 420$nm	4.00	[14]

References

1 H. Liu, J. Meng and J. Zhang, *Catal. Sci. Technol.*, 2017, **7**, 3802-3811.

2 L. Li, G. Liu, S. Qi, X. Liu, L. Gu, Y. Lou, J. Chen and Y. Zhao, *J. Mater. Chem. A*, 2018, **6**, 23683-23689.

3 H. Li, Z. Wang, Y. He, S. Meng, Y. Xu, S. Chen and X. Fu, *J. Colloid Interface Sci.*, 2019, **535**, 469-480.

4 Q. Huang, Y. Xiong, Q. Zhang, H. Yao and Z. Li, *Appl. Catal., B*, 2017, **209**, 514-522.

5 P. Zeng, J. Luo, J. Wang and T. Peng, *Catal. Sci. Technol.*, 2019, **9**, 762-771.

6 J. Wang, J. Luo, D. Liu, S. Chen and T. Peng, *Appl. Catal., B*, 2019, **241**, 130-140.
7 X. Liu, Q. Liu, P. Wang, Y. Liu, B. Huang, E. A. Rozhkova, Q. Zhang, Z. Wang, Y. Dai and J. Lu, *Chem. Eng. J.*, 2018, **337**, 480-487.
8 Y. Liu, Z. Gong, Y. Xie, H. Lv and B. Zhang, *Appl. Surf. Sci.*, 2020, **505**, 144637.
9 Y. Han, X. Dong and Z. Liang, *Catal. Sci. Technol.*, 2019, **9**, 1427-1436.
10 M. Wang, Q. Liu, N. Xu, N. Su, X. Wang and W. Su, *Catal. Sci. Technol.*, 2018, **8**, 4122-4128.
11 Q. Huang, Z. Tao, L. Ye, H. Yao and Z. Li, *Appl. Catal., B*, 2018, **237**, 689-698.
12 R. Chen, Y. Ao, C. Wang and P. Wang, *Dalton Trans.*, 2019, **48**, 14783-14791.
13 X. Liu, X. Liang, P. Wang, B. Huang, X. Qin, X. Zhang and Y. Dai, *Appl. Catal., B*, 2017, **203**, 282-288.
14 H. Liu, Z. Xu, Z. Zhang and D. Ao, *Appl. Catal. A: Gen.*, 2016, **518**, 150-157.